

THEORETICAL &amp; APPLIED MECHANICS LETTERS 4, 051010 (2014)

## Effective thermal conductivity of wire-woven bulk Kagome sandwich panels

Xiaohu Yang,<sup>1</sup> Jiayi Bai,<sup>2</sup> Ki-Ju Kang,<sup>3</sup> Tianjian Lu,<sup>2, a)</sup> Tongbeum Kim<sup>4, b)</sup><sup>1</sup>*School of Energy and Power Engineering, Xi'an Jiaotong University, Xi'an 710049, China*<sup>2</sup>*State Key Laboratory for Mechanical Structure Strength and Vibration, Xi'an Jiaotong University, Xi'an 710049, China*<sup>3</sup>*Department of Mechanical Systems Engineering, Chonnam National University, Gwangju 500-757, South Korea*<sup>4</sup>*School of Mechanical Engineering, University of the Witwatersrand, Johannesburg, Wits 2050, South Africa*

(Received 19 March 2014; revised 25 June 2014; accepted 6 August 2014)

**Abstract** Thermal transport in a highly porous metallic wire-woven bulk Kagome (WBK) is numerically and analytically modeled. Based on topology similarity and upon introducing an elongation parameter in thermal tortuosity, an idealized Kagome with non-twisted struts is employed. Special focus is placed upon quantifying the effect of topological anisotropy of WBK upon its effective conductivity. It is demonstrated that the effective conductivity reduces linearly as the porosity increases, and the extent of the reduction is significantly dependent on the orientation of WBK. The governing physical mechanism of anisotropic thermal transport in WBK is found to be the anisotropic thermal tortuosity caused by the intrinsic anisotropic topology of WBK.

© 2014 The Chinese Society of Theoretical and Applied Mechanics. [doi:10.1063/2.1405110]

**Keywords** effective thermal conductivity, wire-woven bulk Kagome, anisotropy, analytical model

High porosity metallic lattice truss structures (LTSs) have received much attention recently, due to their multi-functional attributes and splendid material efficiency for mechanical loading, thermal management, dynamic load protection, acoustic damping, and so on.<sup>1-3</sup> For instance, in situations where a structure needs to carry both mechanical and thermal load, lattice truss-cored sandwich panels are more attractive than conventional solid materials. Under forced convection, they can be employed for active cooling applications such as jet blast deflector (JBD).<sup>4</sup> When the forced convective flow is stagnant, they may act as thermal protection (insulation), e.g., the skin layer of a re-entry vehicle.<sup>1,2</sup>

Octet, tetrahedral, pyramidal, X-type lattice, three-dimensional (3D)-Kagome and woven structures are presently the main topologies considered for constructing LTSs.<sup>5-8</sup> In particular, the Kagome trusses are regarded as one of the best, due to equivalent elastic stiffness but four times resistance to buckling relative to octet trusses.<sup>8</sup> Recently, Lee et al.<sup>7,9</sup> introduced a new technique for fabricating multilayered metallic Kagome trusses (referred to here as wire-woven bulk Kagome (WBK)) (see Fig. 1) via systematic assembly of helical wires in six directions distributed

<sup>a)</sup>Corresponding author. Email: [tjlu@mail.xjtu.edu.cn](mailto:tjlu@mail.xjtu.edu.cn).

<sup>b)</sup>Corresponding author. Email: [tongkim@wits.ac.za](mailto:tongkim@wits.ac.za).

evenly in 3D space. Distinct from existing methods for fabricating multilayered cellular metals, this type of fabrication is based on stacking node-to-node and bonding of single-layered cellular truss metals, guaranteeing uniform topology, high specific strength, and low cost. The WBK truss shows good performance in compressive strength and energy absorption and outperforms other cellular metals, such as egg box structures, aluminum foams, and woven textile metals.<sup>10</sup> Further, WBK truss has potential for heat dissipation applications due to its flow-through topology, high specific area, high conducting ligaments (e.g., Al) and high flow mixing capability. Therefore, lightweight sandwich constructions with WBK truss cores are expected to perform well when mechanical and thermal loads are simultaneously applied.

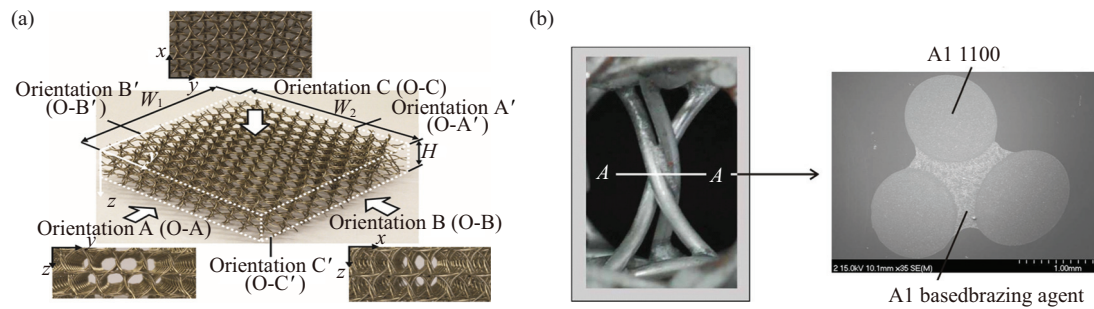


Fig. 1. (a) As-fabricated multilayered, metallic WBK truss structure and three typical orientation views, (b) brazed helical joint of WBK.

For thermal management applications, the effective thermal conductivity (ETC) of cellular metals is a key material property. To estimate the ETC of WBK-cored sandwich constructions, the two-phase (i.e., solid and fluid) truss core may be regarded as a homogenized medium. Maxwell<sup>11</sup> pioneered theoretical modeling of ETC for two-phase porous media where one phase is dispersed in the parent material (continuous phase). However, Maxwell model can not give reasonable estimates when both phases of the porous media are continuous (e.g., WBK truss) in view of its inherent assumptions. To estimating the effective conductivity of porous media with different topologies, a multitude of analytical and numerical studies have been proposed based on Maxwell's pioneering work.<sup>12-15</sup> Idealized assumptions such as random distribution of each phase<sup>16,17</sup> and symmetrical distribution of the two phases<sup>18</sup> were generally used in these studies. However, it has been demonstrated that these models (both analytical and numerical) led to unsatisfactory predictions of ETC for cellular lattice structures<sup>19-22</sup> possibly because of the adopted idealized topologies of porous media.

For lattice frame materials (LFMs), a literature survey<sup>23-25</sup> shows that: (1) existing models for ETC are mainly based on resistance analysis of thermal-electrical networks; (2) thermal resistance modeling can only give a global analysis of heat conduction as well as ETC for LFMs, and hence mechanisms of heat transport at pore levels are not fully explored; (3) little attention is paid on the anisotropic feature of effective conductivity and its physical mechanisms.

Recently, by introducing more realistic topologies, Yang et al.<sup>19-22</sup> investigated analytically and numerically the ETC of high porosity porous media such as cellular foams. One-dimensional (1D) conduction path via solid ligaments of a selected unit cell (UC) was assumed. For sufficiently high porosities (typically  $> 0.9$ ), Yang et al. demonstrated that the effective conductivity

can be expressed as a function of porosity and topological constants related to the length of 1D conduction path. Good agreement was achieved between model predictions and experimental measurements for open-cell metal foams (random topology, isotropic).<sup>19–21</sup> However, as LTSs (including WBK considered in the present study) exhibit in general anisotropic topologies, existing models for effective conductivity of porous media need to be revisited. Further, physical insight into the thermal transport in LTSs has not been sufficiently valued.

We aim to estimate the ETC of metallic WBK truss structures using a combined approach of analytical modeling, experimental measurement, and numerical simulation. The analysis is based on 1D heat conduction through highly-tortuous ligaments of high porosity ( $> 0.9$ ) WBK trusses. The concept of thermal tortuosity is used to investigate microscopically (at pore level) and understand physically the heat conduction paths through the WBK truss structure. Particular focus is placed upon the anisotropic feature and physical mechanisms of heat conduction in WBK.

The WBK truss structure is fabricated by continuous helical wires that are systematically assembled,<sup>7–9</sup> as shown in Fig. 1(a). First, circular metallic (e.g., aluminum) wires, each having diameter of 1 mm, are formed into a helical shape with pitch 14.7 mm and helical radius 0.6 mm. The helical wires are then assembled in six directions to create multi-layered WBK structure. Subsequently, a brazing agent is pasted on each helical joint for bonding (see Fig. 1(b)). For sandwich construction, the WBK truss (as the core) is brazed with two metallic face sheets.

The WBK truss assembled by continuous helical wires has a configuration similar to that of an idealized Kagome truss<sup>7</sup> created using straight struts. Following the tortuosity analysis of Yang et al.<sup>21</sup> the elongation of wires due to twisting results in a reduced effective conductivity relative to that of the ideal Kagome having the same porosity. The reduction ratio may be evaluated by introducing an elongation parameter  $\alpha$ , defined as the length ratio of twisted ligament to straight (non-twisted) ligament. For the as-fabricated aluminum WBK truss structure shown in Fig. 1, the elongation parameter  $\alpha$  is measured to be 1.04, which is small. Hence, for convenience and minimization of computational costs, the idealized Kagome structure is employed below for both analytical modeling and numerical simulation.

For fluid-saturated metallic lattice trusses, the contribution of heat conduction from the fluid phase may be neglected as the thermal conductivity ratio of solid to fluid is usually large, e.g.,  $k_s/k_f > 8000$  for air-saturated aluminum trusses. The transport of heat in such porous media is therefore conducted only through the solid cell ligaments. Further, for sufficiently high porosities, the transport may be taken as 1D along each tortuous slender ligament. Based upon this assumption, Yang et al.<sup>21</sup> demonstrated that the ETC of high porosity porous media may be expressed as a function of porosity and thermal tortuosity as  $k_e/k_s = (1 - \phi)/\tau$ , where  $k_e$  is the effective conductivity of the porous medium,  $k_s$  is the thermal conductivity of the solid ligaments,  $\phi$  is the porosity, and  $\tau$  is the thermal tortuosity that reflects the elongation of heat conducting path within the porous medium. This approach is adopted below to determine analytically the effective conductivity of WBK.

With reference to Fig. 2, by adopting the concept of 1D conduction via wire ligaments,<sup>19,21</sup> the ETC of the present WBK in O-C of the selected UC may be determined as  $k_e/k_s = (H_c/A_0)/(\int_0^{H(s)} [A_L(s)]^{-1} ds)$ , where  $A_0$  and  $H_c$  are the heat transfer area and thickness of the UC, and the heat transfer length via the tortuous ligament in the UC can be calculated as  $\int_0^{H(s)} [A_L(s)]^{-1} ds =$

$8L/(3\pi d^2)$ . With the relative density ( $\rho^* = 1 - \phi$ ) of the UC (and hence the WBK block as a whole) determined as  $\rho^* = 1 - \phi = 3\pi d^2/(4\sqrt{2}L^2)$ , the ETC of the WBK in O-C is finally obtained as  $k_e/k_s = (1 - \phi)/3$ . Compared with  $k_e/k_s = (1 - \phi)/\tau$ , the normalized effective conductivity  $k_e/k_s$  is the product of porosity and a coefficient of  $1/3$ . In other words, the tortuosity  $\tau$  of the WBK along O-C (see Fig. 1) is 3.

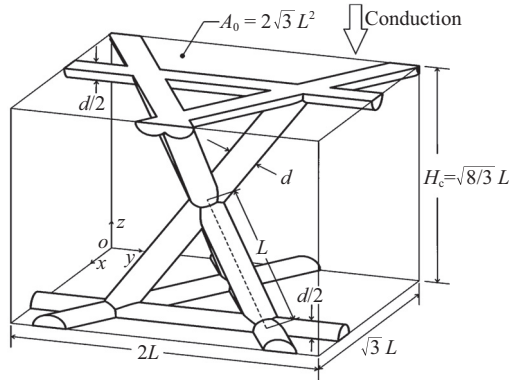


Fig. 2. UC model of idealized Kagome structure having a uniform diameter of circular ligaments,  $d$  and lateral length,  $L$ .

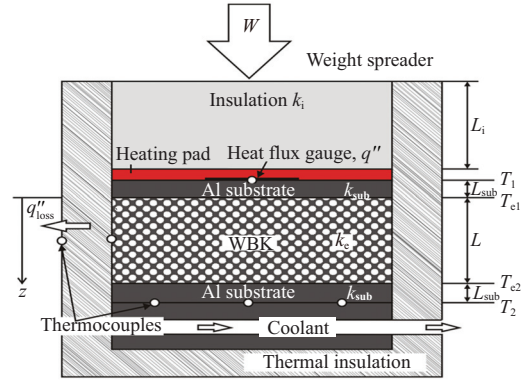


Fig. 3. Schematic of the test rig for ETC measurements with controllable power input and thermostatic bath, with  $z$ -axis coinciding with heat flow direction.

To validate the analytical prediction of  $k_e/k_s = (1 - \phi)/3$ , a purposely-designed test rig is built as illustrated in Fig. 3. A WBK specimen is put into a cubic container made of a low conducting material (Perspex). Heat is applied by an etched-foil heating pad attached to the outer surface of the upper Al substrate, and is thus dominated by conduction from the top through the WBK truss to a cooling system (Contraves Rheotherm 115<sup>TM</sup>) at the bottom.

Surface temperatures  $T_1$  and  $T_2$  are separately measured by K-type thermocouples built-in the film heat flux gauge (Omega<sup>TM</sup>) as well as T-type foil thermocouples (thickness  $13 \mu\text{m}$ , Omega<sup>TM</sup>) attached to the Al substrates. As illustrated in Fig. 3, 1D heat conduction occurs along the  $z$ -axis. The ETC  $k_e$  of the test sample is calculated following Fourier's steady-state heat conduction law, as  $k_e = -q''_{\text{net}}L/(\Delta T)$ , where  $q''_{\text{net}}$  is the net heat flux defined as  $q''_{\text{net}} = q'' - q''_{\text{loss}}$ ,  $L$  is the sample length along the  $z$ -axis (Fig. 3) and  $\Delta T = T_{e2} - T_{e1} = T_2 - T_1$  is the temperature difference between the upper and the lower surfaces of the WBK block.

Quantifying  $k_e$  using the experimental setup of Fig. 3 is affected by the following parameters:  $q''_{\text{net}}$ ,  $T_{e1}$ ,  $T_{e2}$ , and  $L$ . With  $L$  fixed, the errors associated with the measurement of  $k_e$  may be estimated as  $\Delta k_e/k_e = \sqrt{(\Delta q''_{\text{net}}/q''_{\text{net}})^2 + [\Delta T_{e1}/(T_{e1} - T_{e2})]^2 + [\Delta T_{e2}/(T_{e1} - T_{e2})]^2}$ ,<sup>26</sup> where the error associated with the temperatures  $T_{e1}$  and  $T_{e2}$  due to film thermocouple calibration and resolution of the data acquisition device is estimated to be  $0.2^\circ\text{C}$ . For the input heat flux ( $q''_{\text{net}}$ ) measured by the film heat flux gauge, the error stems mainly from signal readings by the multimeter and is estimated to be within 2.0%. Overall, the uncertainty in the present measurement of  $k_e$  is estimated to be less than  $\pm 3.5\%$ .

In addition to experimental measurement, to explore the mechanism of heat transport in the WBK, direct numerical simulations with the finite volume method (FVM) embedded within the commercially available software ANSYS-CFX 14.0 are carried out. A solid geometry is gener-

ated using SOLIDWORKS<sup>TM</sup> as depicted in Fig. 4(a) and then exported to ANSYS-CFX 14.0 for steady-state heat conduction analysis. Constant temperature thermal boundary condition is imposed on the top and the bottom faces (e.g., those perpendicular to O-C, Fig. 4(a)), while the other four faces are kept at adiabatic. To investigate the effect of anisotropic topology on effective conductivity, similar boundary conditions are applied to the WBK block for heat conduction along other selected orientations.

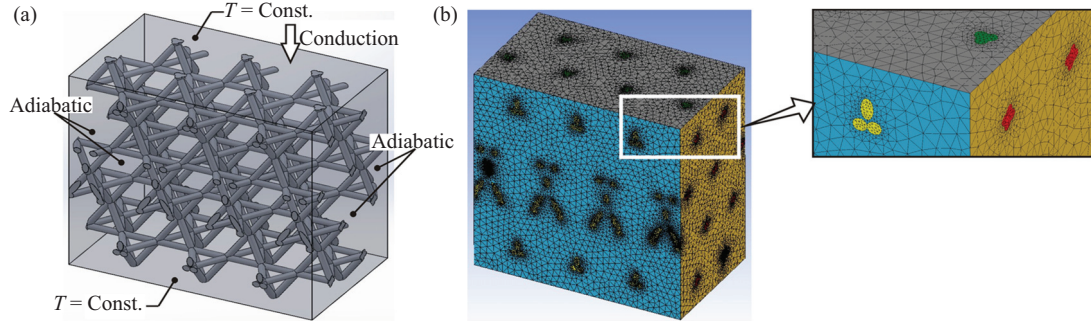


Fig. 4. Numerical model: (a) solid model with thermal boundary conditions for the whole WBK block sample, (b) representative meshes.

In Fig. 5, the normalized ETC ( $k_e/k_s$ ) of air-saturated WBK truss in O-C is plotted as a function of porosity. Within the high porosity range considered ( $\phi \geq 0.90$ ), good agreement is achieved among numerical simulation results, experimental measurements, and analytical model predictions. Through square least fitting, the numerically simulated effective conductivity may be empirically correlated as  $k_e/k_s = -0.34338\phi + 0.34348$ ,  $R^2 = 0.99712$ , where the coefficient 0.34338 represents the reciprocal of thermal tortuosity. Compared with the analytical model of  $k_e/k_s = (1 - \phi)/3$ , the thermal tortuosity resulting from the correlation exhibits a small deviation of  $\sim 3\%$  in the porosity range,  $0.9 \leq \phi \leq 0.98$ . It needs to be noted that a further decrease in porosity leads to ligament thickening for a given pore size, which may violate the assumption of 1D heat conduction along the ligament underlying the present analytical model. Accordingly, it is seen from Fig. 5 that the largest deviation occurs at relatively small porosity levels (around 0.90).

As the WBK truss possesses topological anisotropy, its effective conductivity is expected to

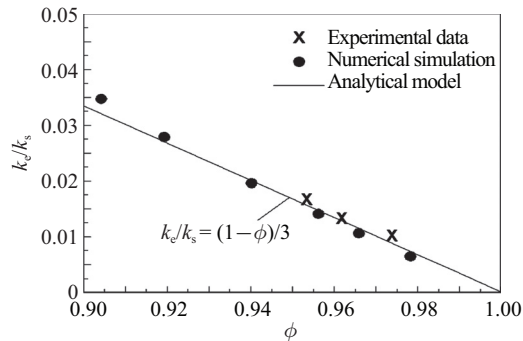


Fig. 5. Comparison of ETC among numerical simulation, experimental measurement, and tortuosity-based analytical model.

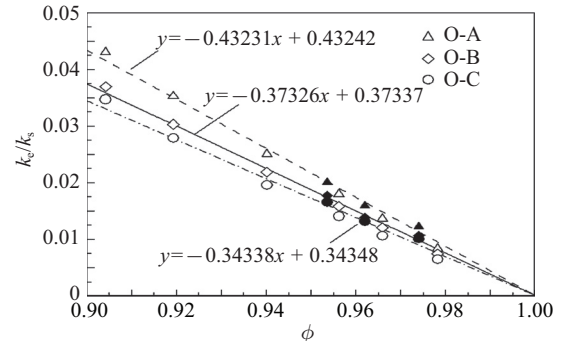


Fig. 6. ETC of WBK along selected orientations. Hollow and solid symbols denote respectively numerical and experimental results.

be anisotropic as well. Figure 6 compares the numerically calculated and experimentally measured effective conductivity of the WBK along three typical orientations. Similar linear trend is observed for the three orientations considered. For a given porosity, O-A has the highest effective conductivity, and this enhancement is more apparent at the lower end of the porosity range ( $0.90 \leq \phi \leq 0.92$ ). As the porosity is increased, the difference of effective conductivity amongst the three orientations becomes smaller. For very high porosities ( $\phi \geq 0.98$ ), the diameter of the metal ligaments is extremely small, e.g., the ligament diameter is only 0.32 mm for  $\phi = 0.99$ . This causes a big thermal resistance, resulting in layered heat conduction in the WBK block and hence the vanishing of the anisotropic feature. Close to the porosity limit of 1, the three lines of effective conductivity in Fig. 6 merge at (0.000 11, 1), 0.000 11 being the thermal conductivity ratio ( $k_f/k_s$ ) of aluminum to air.

Again, based on the least square method, fitting correlations of the numerical results shown in Fig. 6 for O-A and O-B may be obtained as  $k_e/k_s = -0.43231\phi + 0.43242$ ,  $R^2 = 0.99832$  and  $k_e/k_s = -0.37326\phi + 0.37337$ ,  $R^2 = 0.99903$ , where the coefficients 0.373 26 and 0.432 31 imply smaller thermal tortuosity (i.e., smaller heat conduction length) than that in O-C.

So long as the assumption of 1D heat conduction holds, the observed feature of effective conductivity of high-porosity WBK in different orientations is mainly attributed to varying thermal tortuosity induced by varying heat conduction length. A longer heat conduction length leads to a bigger thermal tortuosity and hence, in view of  $k_e/k_s = (1 - \phi)/\tau$ , a smaller effective conductivity. For illustration, consider one representative cut-plane out of the 3D WBK geometry, as shown in Fig. 7, highlighting the imaginary heat conduction path along O-A or O-B. For the present high porosity range ( $\phi \geq 0.90$ ), the ligaments of the Kagome are so thin that 1D-like heat conduction occurs along the ligament (Fig. 7). For O-A, there exists a relatively straight thermal path in the selected UC from high temperature ( $T_H$ ) to low temperature ( $T_L$ ), see Fig. 7(b). For O-B, however, the heat flow path becomes more tortuous, yielding a bigger thermal tortuosity, see Fig. 7(b).

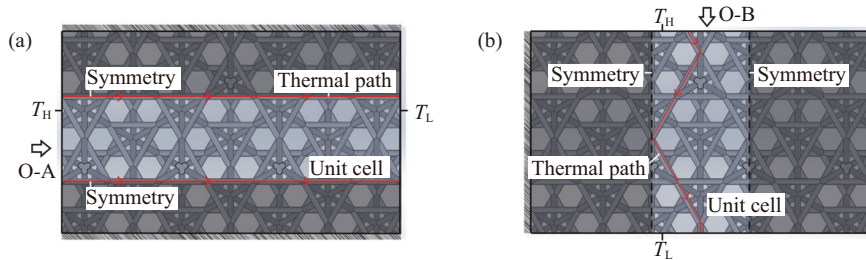


Fig. 7. Imaginary heat conduction path along orientations (a) O-A and (b) O-B.

It should be pointed out that the present analysis of heat conduction physics was carried out on the basis of numerical simulations through large-scale computations. While these computations may be helpful for the design of sandwich panels for multi-functional applications, the computational cost would significantly reduce if spatially periodic computations on a periodic UC of the WBK truss are performed. Such an approach was demonstrated by Albalbaki and Hill<sup>27</sup> to predict water vapor permeability of porous media and will be explored in future studies concerning the effective properties of periodic porous media.

In summary, the ETC of high-porosity, fluid-saturated metallic WBK truss structures is in-

vestigated both numerically and analytically. With the effect of ligament twisting considered by introducing an elongation parameter in thermal tortuosity, a 3D idealized Kagome having straight ligaments is employed for developing both the analytical and the numerical models. Good agreement is achieved between analytical model predictions and numerical simulations. Through least square fitting, the effective conductivity as a function of porosity exhibits a linear trend, with the coefficient of linearity reflecting simply the thermal tortuosity. The intrinsic anisotropic topology of the WBK causes anisotropic heat transport behaviors along different orientations.

*This work was supported by the National 111 Project of China (B06024) and the National Basic Research Program of China (2011CB610305).*

1. T. J. Lu, D. P. He, C. Q. Chen, et al. The multi-functionality of ultra-light porous metals and their applications. *Advances in Mechanics* **36**, 517–535 (2006) (in Chinese).
2. A. G. Evans, J. W. Hutchinson, N. A. Fleck, et al. The topological design of multifunctional cellular metals. *Progress in Materials Science* **46**, 309–327 (2001).
3. T. J. Lu, T. Liu, Z. C. Deng. Multifunctional design of cellular metals: A review. *Mechanics in Engineering* **30**, 1–9 (2008) (in Chinese)
4. T. Kim, H. P. Hodson, T. J. Lu. Fluid-flow and endwall heat-transfer characteristics of an ultralight lattice-frame material. *International Journal of Heat and Mass Transfer* **47**, 1129–1140 (2004).
5. L. J. Gibson, M. F. Ashby. *Cellular Solids: Structure and Properties*. Cambridge University Press, Cambridge (1999).
6. Q. C. Zhang, Y. J. Han, C. Q. Chen, et al. Ultralight X-type lattice sandwich structure (I): Concept, fabrication and experimental characterization. *Science in China Series E: Technological Science* **52**, 2147–2154 (2009).
7. Y. H. Lee, B. K. Lee, I. Jeon, et al. Wire-woven bulk Kagome truss cores. *Acta Materialia* **55**, 6084–6094 (2007).
8. S. Hyun, A. M. Karlsson, S. Torquato, et al. Simulated properties of Kagome and tetragonal truss core panels. *International Journal of Solids and Structure* **40**, 6989–6998 (2003).
9. K. J. Kang. A wire-woven cellular metal of ultrahigh strength. *Acta Materialia* **57**, 1865–1874 (2009).
10. B. K. Lee, K. J. Kang. A parametric study on compressive characteristics of wire-woven bulk Kagome truss cores. *Composite Structure* **92**, 445–453 (2010).
11. J. C. Maxwell. *A Treatise on Electricity and Magnetism*, Vol. 1. Clarendon Press, Oxford (1881).
12. R. Progelhof, J. Throne, R. Ruetsch. Methods for predicting the thermal conductivity of composite systems: a review. *Polymer Engineering & Science* **16**, 615–625 (1976).
13. E. Tsotsas, H. Martin. Thermal conductivity of packed beds: a review. *Chemical Engineering and Processing: Process Intensification* **22**, 19–37 (1987).
14. Z. Hashin, S. Shtrikman. On some variational principles in anisotropic and nonhomogeneous elasticity. *Journal of the Mechanics and Physics of Solids* **10**, 335–342 (1962).
15. H. Russell. Principles of heat flow in porous insulators. *Journal of the American Ceramic Society* **18**, 1–5 (1935).
16. R. Landauer. Electrical resistance of disordered one-dimensional lattices. *Philosophical Magazine* **21**, 863–867 (1970).
17. S. Kirkpatrick. Percolation and conduction. *Reviews of Modern Physics* **45**, 574–588 (1973).
18. C. Hsu, P. Cheng, K. Wong. Modified Zehner–Schlunder models for stagnant thermal conductivity of porous media. *International Journal of Heat and Mass Transfer* **37**, 2751–2759 (1994).
19. X. H. Yang, J. J. Kuang, T. J. Lu, et al. A simplistic analytical unit cell based model for the effective thermal conductivity of high porosity open-cell metal foams. *Journal of Physics D: Applied Physics* **46**, 255302 (2013).
20. X. H. Yang, J. X. Bai, H. B. Yan, et al. An analytical unit cell model for the effective thermal conductivity of high porosity open-cell metal foams. *Transport in Porous Media* **102**, 1–24 (2014).
21. X. H. Yang, T. J. Lu, T. Kim. Thermal stretching in two-phase porous media: Physical basis for Maxwell model. *Theoretical and Applied Mechanics Letters* **3**, 021011 (2013).
22. X. H. Yang, T. J. Lu, T. Kim. Effective thermal conductivity modelling for closed-cell porous media with analytical shape factors. *Transport in Porous Media* **100**, 211–224 (2013).
23. Z. G. Qu, T. S. Wang, W. Q. Tao, et al. A theoretical octet-truss lattice unit cell model for effective thermal conductivity of consolidated porous materials saturated with fluid. *Heat Mass Transfer* **48**, 1385–1395 (2012).
24. H. N. G. Wadley. Multifunctional periodic cellular metals. *Phil. Trans. R. Soc. A* **364**, 31–68 (2006).
25. G. Sun, L. Gao. Heat transfer characteristics of composite sandwich structure with lattice cores. *Acta Materialia Compositae Sinica* **28**, 185–195 (2011).
26. H. W. Coleman, W. G. Steele. *Experimentation, Validation, and Uncertainty Analysis for Engineers*. John Wiley & Sons Incorporated, New York (2009).
27. B. Albalbaki, R. J. Hill. Computational implementation of interfacial kinetic transport theory for water vapour transport in porous media. *Proc. R. Soc. A: Math. Phys. Eng. Sci.* **470**, 20130278 (2014).